# Radionuclide Computed Tomography of the Body Using Routine Radiopharmaceuticals. II. Clinical Applications

John A. Burdine, Paul H. Murphy, and E. Gordon DePuey

*Baylor College of Medicine, and St. Luke's Episcopal-Texas Children's Hospitals, Houston, Texas*

***A whole-body computed tomography system for single-photon emitters was used to investigate the clinical utility of this imaging modality. We have explored its application in brain, lung, liver, kidney, cardiac, bone, and gallium imaging in over 200 patients. Brain images demonstrated better lesion contrast than that in standard scintiphotos. Images of the lung and liver showed radionuclide distribution that was not readily apparent in standard scintiphotos. Moderate or strongly positive pyrophosphate myocardial images demonstrate the potential for infarct quantitation. ECG-gated cardiac blood-pool images in cross section, displayed in cine formate, permit evaluation of segmental motion of the free and septal walls of both ventricles. These results suggest significant clinical potential for this imaging modality using standard radiopharmaceuticals, but some increase in system sensitivity will likely be necessary to realize the full benefit of the technique.***

**J Nucl Med 20: 108–114, 1979**

Stimulated by encouraging results in a previously reported pilot study using a radionuclide emission computed tomographic (ECT) instrument designed for the head (*1*), a "tunnel" version of this ECT device was constructed for body imaging using two large-field-of-view scintillation cameras. The system resolution is relatively constant through the scanned volume at 16.5 mm as measured by the FWHM for Tc-99m in air, and the sensitivity in air is 10.6 cps/$\mu$Ci (*2*). The cameras rotate in a gantry about the long axis of the patient at variable speeds so that data collection during a single 360° revolution requires 2-22 min at the discretion of the operator. A series of phantom images demonstrated satisfactory resolution of "hot" and "cold" lesions that were greater than 1.0 cm in diameter. The phantom that was used simulated the volume distribution of an average patient's thorax or abdomen. Although internal attenuation of photons did produce a quantitative change in the apparent activity distribution within the image matrix, the effect on lesion recognition in the clinical images was considerably less than anticipated, with the attenuation correction programs virtually eliminating any observable influence. Based on these observations, a clinical evaluation of the instrumentation and technique was undertaken. The results of brain, lung, liver, kidney, cardiac, bone, and gallium imaging in 200 patients form the basis for this report.

Received Aug. 1, 1978; revision accepted Oct. 13, 1978.

For reprints contact: John A. Burdine, Nuclear Medicine Sec., Dept. of Radiology, Baylor College of Medicine, Houston, TX 77030.

## METHODS

Patients were selected from those referred for various imaging procedures with a standard scintillation camera, and the ECT study was performed subsequently. All studies were accomplished using either Tc-99m-labeled radiopharmaceuticals, Ga-67, or Tl-201. Data-collection times averaged near

the maximum (i.e., 22 min), unless it could not be tolerated by the patient. With the sensitivity limits of the current system, image quality was usually improved in all types of studies if a greater information density was obtained. The thickness of the reconstructed tomographic slices was arbitrarily limited to either 2.5 cm or 1.25 cm. The 1.25-cm thickness would theoretically be preferred for smaller organs (i.e., kidney and heart) to obtain better anatomic detail, but the resultant decrease in count density produces information density less than optimum in some patients, even with a 22-min imaging time.

In all patients the camera heads were brought into as close apposition as possible, to maximize resolution. The limiting constraint during imaging of the thorax and abdomen was the patient's arms and shoulders, which cannot readily be removed from the field of view with this gantry. The arms were strapped to the abdomen to minimize the cross-sectional area, but this still left a substantial space between the patient and the detectors when they were oriented in the sagittal planes. This circumstance undoubtedly resulted in degradation of image quality as well as an increase in attenuation, but a patient is unable to hold the arms over the head during long imaging times.

## RESULTS

In images of the brain, the definition of normal anatomic detail was judged to be superior in comparison with standard camera scintiphotos that were obtained using parallel-hole or converging collimation. As in the pilot study with the head unit (*1*,*3*), lesion contrast was improved and the interpreter encountered no significant problem in relating the multiple transverse sections to the patient's vertical axis (Fig. 1). One of the theoretical benefits of cross-sectional tomography is its potential for separating intracerebral from extracerebral lesions (*4*) (Fig. 2). With relatively thick slices encompassing a rapidly curving surface, "hot" lesions near the superior or inferior margins of a slice could under certain circumstances be projected somewhat internally despite exclusive confinement to the skull. A specific clinical instance of this effect was suspected but not documented. With the use of thin or overlapping slices and a quasi three-dimensional display, it should be possible to minimize or entirely avoid this potential problem.

The lung-perfusion studies produced a problem that we did not fully anticipate. In carefully reviewing the cross-sectional images in comparison with the standard scintiphotos, we concluded that the ECT lung images contained considerably more in-

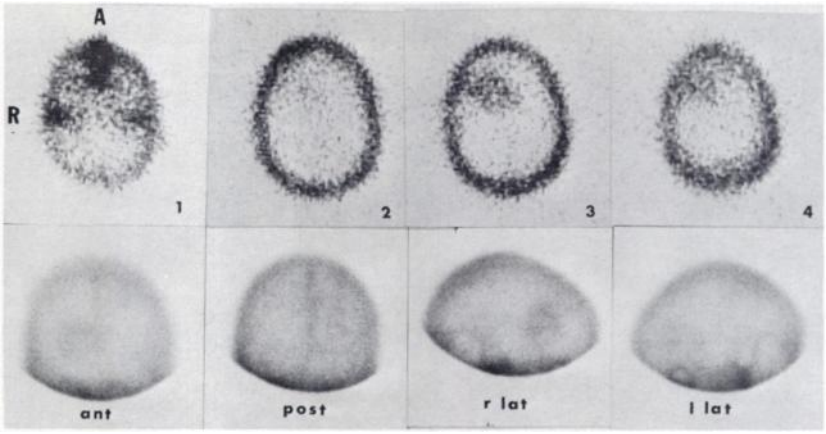


**FIG. 1.** Twenty-one-year-old male with headache and hypovascular frontal lesion. 2.5-cm ECT sections (top) using all-purpose collimators demonstrate improved lesion contrast compared with standard scintiphotos with large field camera (bottom). ECT sections begin numerically with most inferior image, with patient's anterior at the top, and right side at viewer's left. Each image contains approximately 600 thousand counts obtained following 11 min of data collection after administration of 16.5 mCi of Tc-99m pertechnetate.

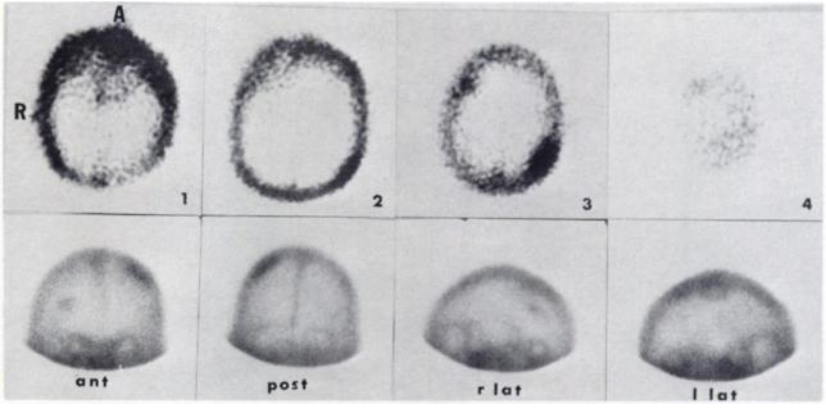


**FIG. 2.** Seventy-eight-year-old woman with breast cancer and dizziness. In ECT images obtained with fan-beam collimators (top), anterior lesion appears to extend internally from skull. This may or may not represent projection artifact. Each image contains approximately 500 thousand counts obtained during 22 min of data collection following the administration of 20.3 mCi of Tc-99m pertechnetate. Standard scintiphotos (bottom) were obtained with large-field camera and converging collimation.

formation concerning the distribution of perfusion, but it was difficult and tedious to assimilate the data from multiple sections into an overall perspective (Fig. 3). In addition, normal anatomic indentations at the surface of the lung were at times hard to separate from lesions. This problem of expanded image data content was also encountered to a lesser extent in the liver-spleen images, and therefore relates mainly to organs with a complex peripheral and internal structure in which the lesions are "cold."

In reviewing the liver images, we noted in the transverse sections some structures that created an initial question of anatomic correspondence. For example, the images shown in Fig. 4 demonstrate in the region of the porta hepatis a defect that extends throughout the liver substance. An unusually prominent porta hepatis is not observed on the standard scintillation-camera views, and it may be that the defect in the ECT slice is created by merging of the ligamentum teres with the porta hepatis in the central portion of the liver. Several presumably normal patients showed a similar pattern, suggesting that ECT imaging has a unique potential for examing the internal structure of the liver.

Figure 5 illustrates the effects of the attenuation-correction algorithms (*5*) on the liver image in a patient with multiple foci of metastatic carcinoma. Note that the effects of attenuation are most prominent toward the center of the ECT section, as indicated by relative decrease in count density. Following attenuation correction, a redistribution of count density occurs so that the central decrease is no longer apparent. In this particular case, all of the lesions were probably visible in the uncorrected images, but lesion-to-background contrast was improved by attenuation correction, and it is likely that recognition of lesions at the threshold of perception would be enhanced through application of correction programs.

The cardiac studies included Tl-201, Tc-99m pyrophosphate, and gated blood-pool images obtained

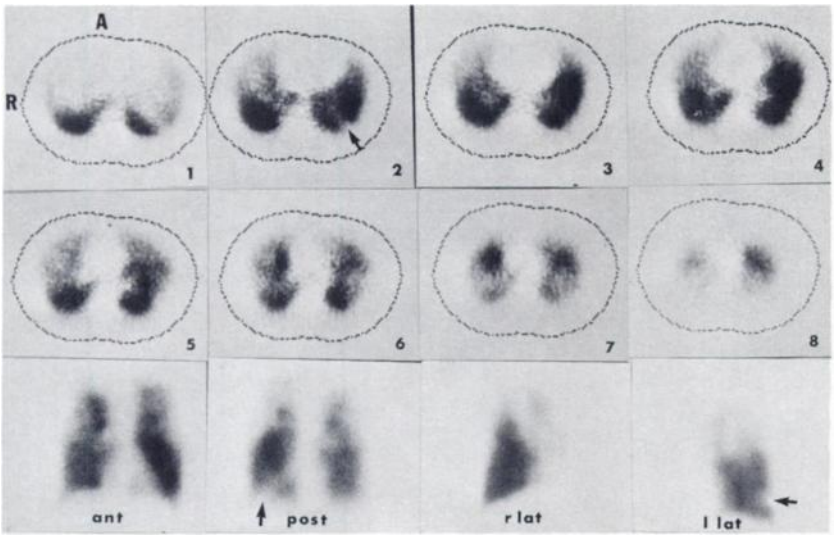


**FIG. 3.** Thirty-two-year-old man with eosinophilic granuloma of lung. Multiple perfusion defects are present in both lungs, and can be seen in ECT and standard scintiphoto images. Patient received 4.0 mCi of Tc-99m MAA. ECT images, obtained with all-purpose collimators and 8 min of data collection, contain approximately 1.2 million counts. Note specifically small defect involving lower posterior surface of left lung (arrows). Perspective of overall lung perfusion is more difficult to obtain from individual ECT sections.

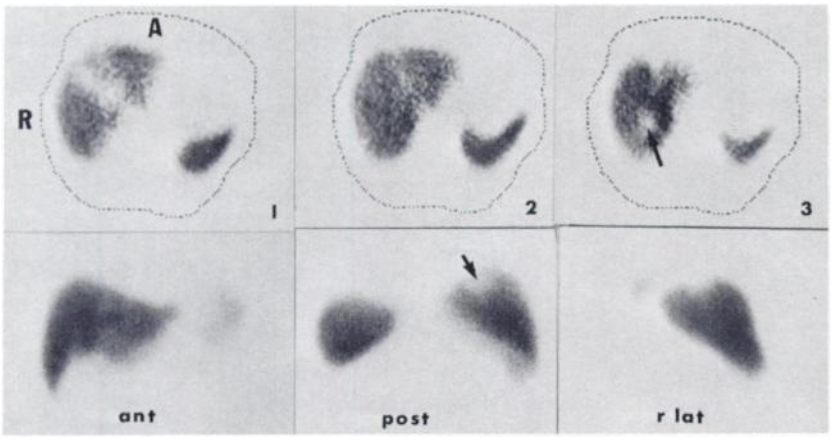


**FIG. 4.** Forty-four-year-old man with carcinoma of colon was scanned for 22 min with high-resolution collimators. ECT images show prominent defect in region of porta hepatis not demonstrated in standard scintiphotos. Also, note space-occupying lesion at the posterosuperior aspect of liver (arrows). ECT images contain approximately 2.9 million counts from 4.7 mCi of Tc-99m sulfur colloid.

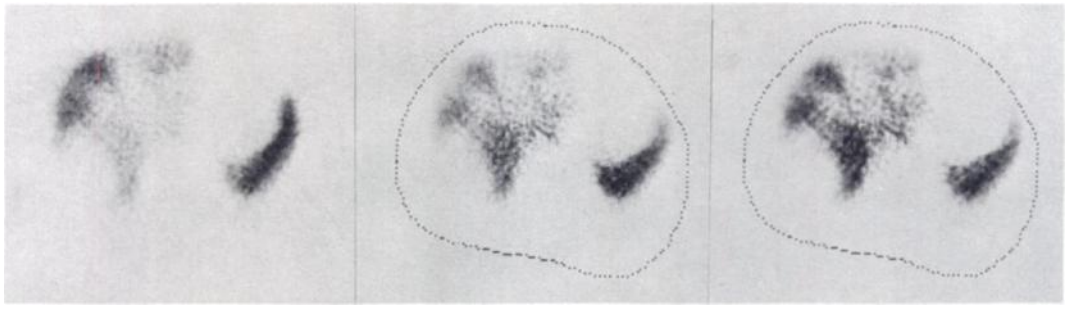

**FIG. 5.** Sixty-three-year-old man with metastatic cancer from unknown primary. Influence of two attenuation-correction algorithms is demonstrated. Uncorrected image is at left. First level of attenuation correction (center) improves lesion contrast and compensates for progressive decrease in intensity towards center of the image. Addition of iterative correction (right) further improves edge definition. Scan time was 22 min following administration of 3.5 mCi of Tc-99m sulfur colloid with high-resolution collimators. Counts per section are approximately 1.1 million.

with Tc-99m albumin. The thallium studies were disappointing in terms of definition of the myocardium (*6*), and this probably was due to inadequate count density (Fig. 6). Since the thallium images were obtained routinely with the system's maximum collection time (22 min), it was not possible to consider longer imaging intervals.

The moderate or strongly positive pyrophosphate images (Fig. 7) provided an opportunity for quantitation of infarct size and have significant clinical potential even with this prototype instrument. We have previously reported this application in dogs using a prototype system (*1*). The borderline positive abnormalities were not seen as well with the ECT system as with the standard camera views, further suggesting the need for increased sensitivity.

Software routines were developed to obtain gated cardiac blood-pool images and display them in cine format. As demonstrated in Fig. 8, the motion of the free and septal walls of both ventricles can be observed simultaneously with this technique. This approach offers an alternative to first-pass ventricular studies as an effective means of avoiding overlapping blood pools (*7*).

We also obtained cross-sectional images of Ga-67 distributions in the abdomen and thorax, bone images with Tc-99m pyrophosphate, and the kidneys and bladder with Tc-99m DTPA. The gallium images were generally low in information density and thus somewhat disappointing, but some areas of increased activity were better defined than in the standard scintiphotos. Since this instrument had only a single pulse-height analyzer, a twofold increase in sensitivity for gallium would be anticipated with the installation of additional analyzers. Cross-sectional bone images of the pelvis were interesting from an anatomic standpoint but in a limited series showed no abnormal areas of tracer concentration not seen with the standard camera. Cross-sectional renal images produced a clear separation between the collection system and the renal parenchyma, and have excellent clinical potential for a more precise location of lesions (Fig. 9).

## DISCUSSION

Emission computed tomography has been under study for several years, primarily because of the technique's unique potential for improvement in the contrast of structures compared with that of conventional planar views (*8–11*). Two distinct lines of

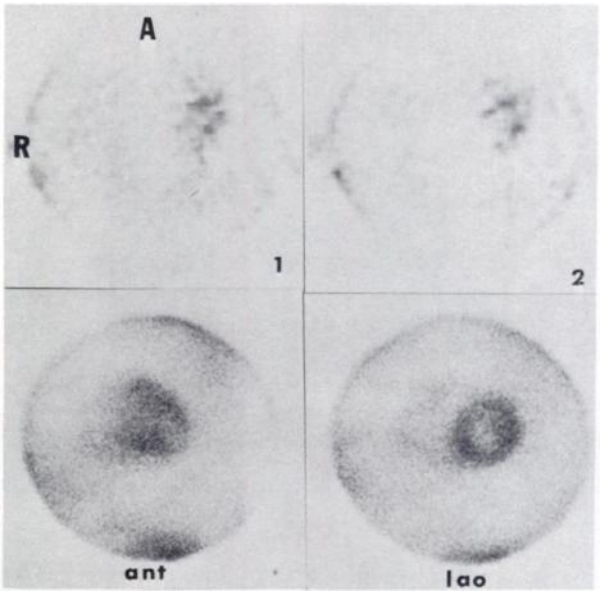


**FIG. 6.** Normal Tl-201 images in a 50-year-old man. Poor quality of ECT sections is due to low count density, in spite of 22 min of data-collection time. Patient received 2.0 mCi of Tl-201 and was imaged with the high-resolution collimators to obtain approximately 130 thousand counts per image. Improvement in system sensitivity would be very beneficial during imaging under conditions of limited photon yield.

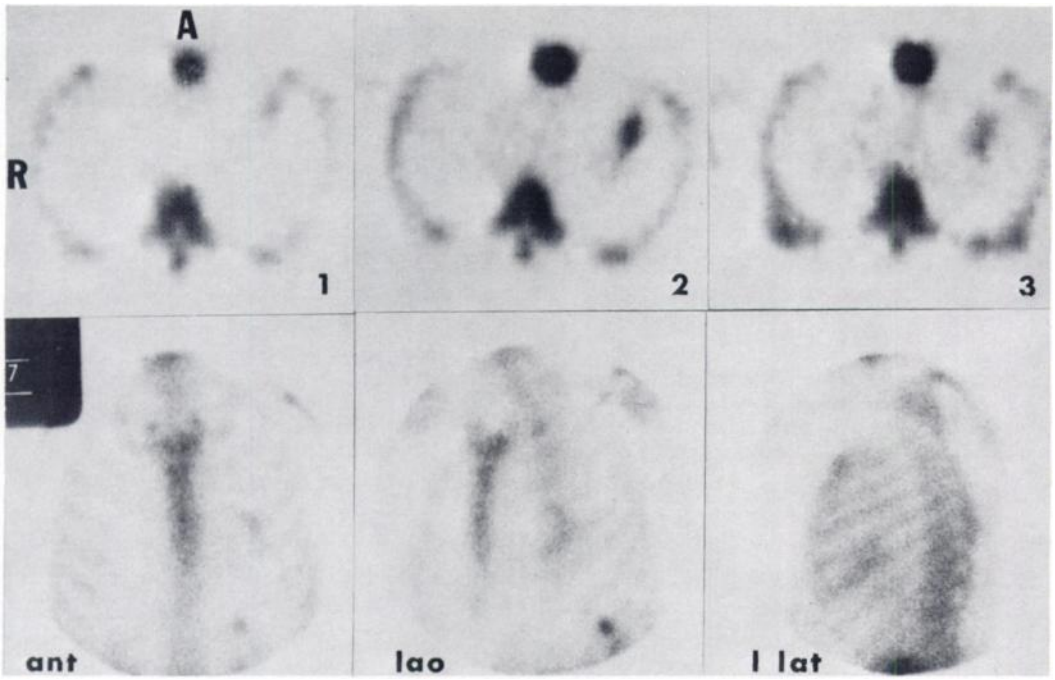


**FIG. 7.** Fifty-two-year-old man with anterolateral myocardial infarct. Technetium-99m pyrophosphate uptake is evident in three adjacent 2.5-cm ECT sections. Based upon this distribution, volume of infarcted tissue was calculated to be 63 cc. Imaging time of 22 min with high-resolution collimator resulted in approximately 1.2 million counts per image after administration of 16.0 mCi of Tc-99m PYP.

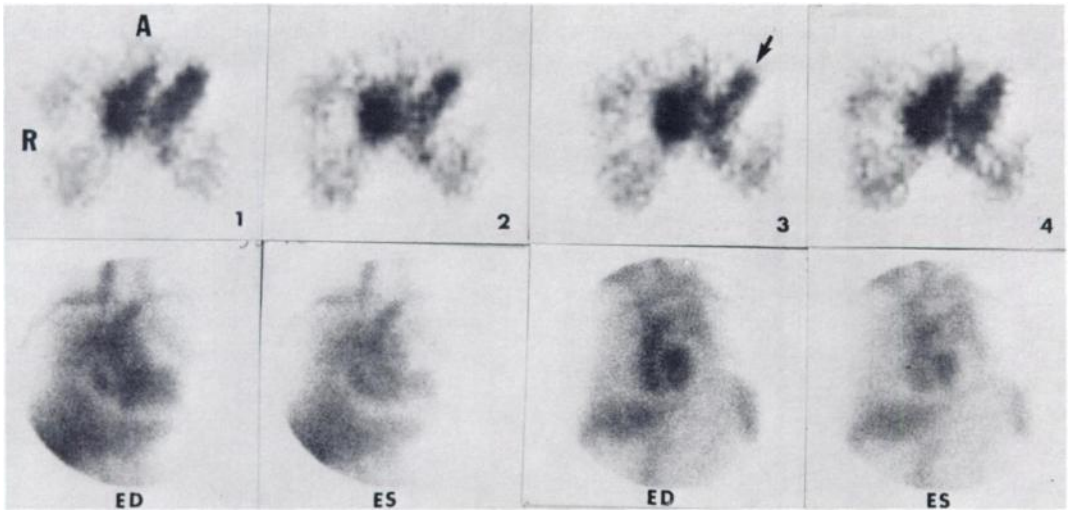


**FIG. 8.** Forty-one-year-old man with left ventricular aneurysm (arrow). ECT image obtained with all-purpose collimators are all at same anatomic level, and constitute four of nine frames of ECG-gated composite cardiac cycle. Images are displayed in cine format, providing visualization of all of walls of both ventricles. Patient received 25.0 mCi of Tc-99m human serum albumin and was scanned for 22 min to yield 840 thousand counts per image.

development have proceeded simultaneously. One of them uses the 511-keV annihilation photons from positron-emitting radionuclides. The fixed spatial and temporal relationship between the two annihilation photons permits transverse-section reconstructions of the radionuclide distribution. The second line of pursuit centers around single-photon emitters. This emission distribution is measured at several projection angles around the object, and with computer reconstruction algorithms similar to those used in positron and x-ray computed tomography, transverse sections of the radionuclide distribution can be developed.

Comparison of the two methods indicates that

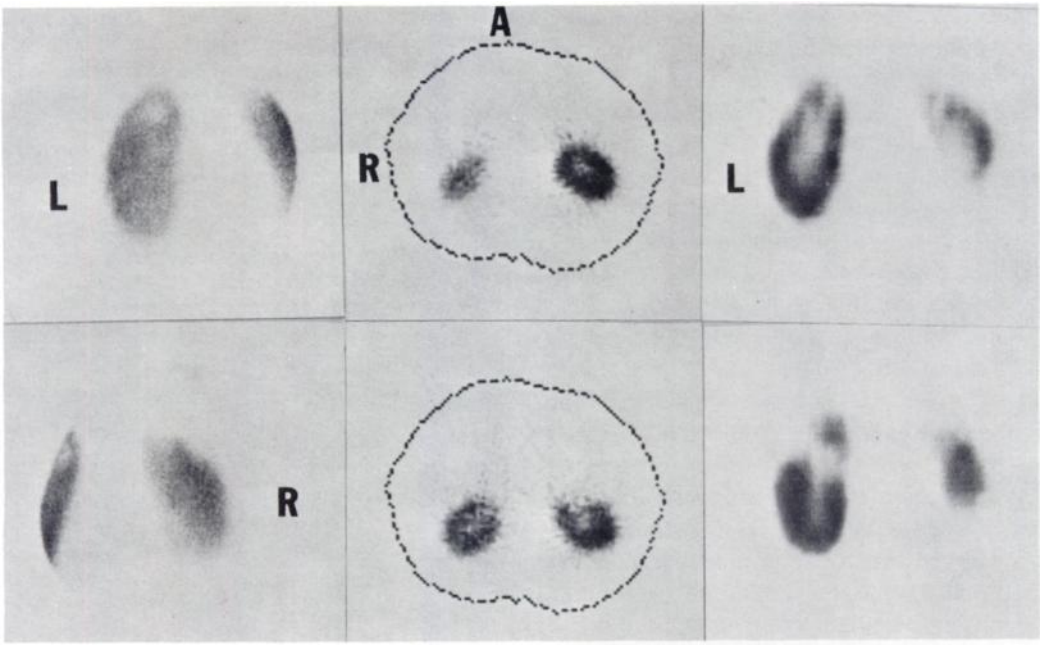


**FIG. 9.** Seventy-three-year-old woman with hypertension and caliectasis. Extent of caliceal dilation is more prominent in longitudinal sections (right), but separation of collection system from the renal parenchyma is better seen on transverse sections (center). High-resolution collimators were used for this 11-min scan at three hr postinjection yielding 800 thousand counts per image from injection of 10.8 mCi of Tc-99m DTPA.

each has advantages and disadvantages. The positron technique has the potential for the generation of new and clinically relevant information by using positron-emitting isotopes of oxygen, nitrogen, and carbon as labels for the analysis of fundamental substrate pathways (*12–17*). On the other hand, a major advantage of single-photon ECT is the applicability of standard medium- and low-energy radiopharmaceuticals, which are widely available compared with the cyclotron-produced positron emitters. For both techniques accurate attenuation correction is mandatory to obtain quantitative results, in terms of activity per unit volume. Theoretically, accurate attenuation correction can be obtained with either method, but it is far more difficult to implement in a practical sense with the single-photon emitters. In the positron case, attenuation is a function of the total thickness of the object along a given ray, whereas in the single-photon case attenuation varies from cell to cell with the distribution of the radionuclide along a ray. Also, the higher energy annihilation photons result in smaller changes in the attenuation coefficient throughout the object than those usually encountered with the lower gamma-ray energies emitted from most radionuclides used in single-photon studies. Budinger has discussed eight different methods for single-photon attenuation correction (*18*) and concludes that the techniques are generally superior for the higher energy photon emitters and quantitative results to an accuracy of within 10% can be obtained. For an object of known geometry, better results can be obtained as has been demonstrated by Kuhl (*19*).

The basic mechanical configuration of the ECT device used in this investigation was not designed to be optimal for clinical studies, but instead to permit evaluation of the technique with maximum flexibility of computer processing in relation to the data-collection and display routines. With some mechanical engineering redesign, it is quite feasible to create a system that would perform all of the basic imaging functions of a large-field camera including biplane imaging, total-body imaging, and the selective use of tomography, both transverse and longitudinal. An improvement in sensitivity would be necessary, both to shorten imaging time and, more importantly, to increase the information density of the images, particularly the 1.25-cm thick slices and the count-poor studies such as those obtained with Ga-67, Tl-201, and Tc-99m pyrophosphate. Further refinement in collimation has an immediate potential for increasing sensitivity, but it is possible that a different detector design involving greater geometric efficiency will be necessary before the full potential of this imaging modality is realized. The massive data in 8-10 ECT sections in comparison with the usual number of standard scin-

tiphotos, create an interesting challenge for the development of an interactive display. To make it easier for the interpretor to gain an overall perspective of the organ, an operator-controlled three-dimensional or other composite display would be beneficial. In view of the basic data that are available for reconstruction, it is possible to obtain not only a three-dimensional display, but also to construct composite two-dimensional images from any plane, and to select areas of interest for detailed transverse or longitudinal tomographic analysis. Such capabilities are not inconsistent with the current state of technology (*20*).

Because of recent national and state legislation, any medical device exceeding $100,000 in cost must pass a cost-effectiveness threshold in terms of offering to the clinician substantial information that is not available through other less costly or safer modalities. Taking into consideration the advances in x-ray computed tomography and ultrasound and adding the improvement in imaging capabilities of standard scintillation cameras including post imaging processing, we find it difficult to define the ultimate potential of single-photon ECT at this time. This initial evaluation of a body ECT device using standard radiopharmaceuticals consistently produced clinical information that was not available or as easily discerned from the standard scintiphotos. Nevertheless, although single-photon whole body ECT has demonstrated great promise and continued development should be accomplished, until a significant increase in sensitivity can be achieved, inadequate count density will hamper the clinical effectiveness of this modality.

ACKNOWLEDGMENTS

We are most grateful for the helpful comments and advice of the following consultants: Alexander Gottschalk, M.D., Robert Henkin, M.D., John Keyes, M.D., Wil Nelp, M.D., Barry Siegel, M.D., and Paul Weber, M.D.

This paper was presented in part at the 25th Annual Meeting of the Society of Nuclear Medicine, 1978, Anaheim, CA.

REFERENCES

1. JASZCZAK RJ, MURPHY PH, HUARD D, et al: Radionuclide emission computed tomography of the head with $^{99m}$Tc and a scintillation camera. *J Nucl Med* 18: 373–380, 1977
2. MURPHY PH, THOMPSON WL, MOORE ML, et al: Radionuclide computed tomography of the body using routine radiopharmaceuticals: I. System characterization. *J Nucl Med:* in press
3. DENDY PP, MCNAB JW, MACDONALD AF, et al: An evaluation of transverse axial emission tomography of the brain in the clinical situation. *Br J Radiol* 50: 555–561, 1977
4. KEYES JW JR, ORLANDEA N, HEETKERKS WJ, et al: The humongotron—a scintillation-camera transaxial tomograph. *J Nucl Med* 18: 381–387, 1977
5. CHANG LT: A method for attenuation correction in radionuclide computed tomography. *IEEE Trans Nucl Sci* NS-25: 638–643, 1978
6. KEYES JW JR, LEONARD PF, SVETKOFF DJ, et al: Myocardial imaging using emission computed tomography. *Radiology* 127: 809–812, 1978
7. BUDINGER TF, CAHOON JL, DERENZO SE, et al: Three dimensional imaging of the myocardium with radionuclides. *Radiology* 125: 433–439, 1977
8. KUHL DE, EDWARDS RQ: Image separation radioisotope scanning. *Radiology* 80: 653–661, 1963
9. TER-POGOSSIAN MM: Basic principles of computed axial tomography. *Semin Nucl Med* 7: 109–127, 1977
10. PHELPS ME: Emission computed tomography. *Semin Nucl Med* 7: 337–365, 1977
11. PHELPS ME: What is the purpose of emission computed tomography in nuclear medicine? *J Nucl Med* 18: 399–402, 1977
12. SOBEL BE, WEISS ES, WELCH MJ, et al: Detection of remote myocardial infarction in patients with positron emission transaxial tomography and intravenous $^{11}$C-palmitate. *Circulation* 55: 853–857, 1977
13. GALLAGHER BM, ANSARI A, ATKINS H, et al: Radiopharmaceuticals XXVII. $^{18}$F-labeled 2-deoxy-2-fluoro-D-glucose as a radiopharmaceutical for measuring regional myocardial glucose metabolism in vivo: Tissue distribution and imaging studies in animals. *J Nucl Med* 18: 990–996, 1977
14. WEISS ES, AHMED SA, WELCH MJ, et al: Quantification of infarction in cross sections of canine myocardium in vivo with positron emission transaxial tomography and $^{11}$C-palmitate. *Circulation* 55: 66–73, 1977
15. TER-POGOSSIAN MM, WEISS ES, COLEMAN RE, et al: Computed tomography of the heart. *Am J Roentgenol* 127: 79–90, 1976
16. PHELPS ME, HOFFMAN EJ, COLEMAN RE, et al: Tomographic images of blood pool and perfusion in brain and heart. *J Nucl Med* 17: 603–612, 1976
17. CROCKER EF, ZIMMERMAN RA, PHELPS ME, et al: The effect of steroids on the extravascular distribution of radiographic contrast material and technetium pertechnetate in brain tumors as determined by computed tomography. *Radiology* 119: 471–474, 1976
18. BUDINGER TF, GULLBERG GT: Transverse section reconstruction of gamma-ray emitting radionuclide in patients. In *Reconstruction Tomography in Diagnostic Radiology and Nuclear Medicine*, Ter-Pogossian MM, Phelps ME, Brownell GL, et al, eds. Baltimore, Md, University Park, 1977, pp 315–341
19. KUHL DE, EDWARD RQ, RICCI AR, et al: The Mark IV system for radionuclide computed tomography of the brain. *Radiology* 121: 405–413, 1976
20. GLENN WV, JOHNSTON RJ, MORTON PE, et al: Image generation and display techniques for CT scan data. Thin transverse and reconstructed coronal and sagittal planes. *Invest Radiology* 10: 403–416, 1975